Improving optical properties of white light-emitting diodes using triple-layer remote structure

Thanh Binh Ly[1], Phan Xuan Le[2]

[1]Faculty of Fundamental Science, Industrial University of Ho Chi Minh City, Ho Chi Minh City, Vietnam
[2]Faculty of Mechanical-Electrical and Computer Engineering, School of Engineering and Technology, Van Lang University, Ho Chi Minh City, Vietnam

Article Info

ABSTRACT

In recent efforts to improve the performance of white light-emitting diode (WLEDs), researchers have focused on angular color uniformity (ACU), an effective index for evaluating the light quality of WLEDs. In this article, we also aim for the WLED development by applying three phosphor layers in the remote phosphor structure. The dual-layer phosphor (DLP) remote structure is also included in the research for comparison with the triple-layer phosphor (TLP) in terms of their impacts on the lighting quality of WLEDs. To ensure the diversity and applicability in different scenarios, performances of multi-layer phosphor structures in WLED devices with average correlated color temperatures (ACCTs) from 5,600 K to 8,500 K are measured. The experimental results have proved that both TLP and DLP structures are suitable to enhance WLEDs' performance as each structure excels at specific qualities. In particular, at all ACCTs, the DLP structure is getting better in improving the color rendering index (CRI), while the TLP is more advantageous to color quality scale (CQS) and light output. The TLP also presents a lower color deviation than the DLP does, which leads to a better color uniformity in WLEDs at all ACCTs.

Corresponding Author:

Phan Xuan Le
Faculty of Mechanical-Electrical and Computer Engineering, School of Engineering and Technology,
Van Lang University
Ho Chi Minh City, Vietnam
Email: le.px@vlu.edu.vn

1. INTRODUCTION

The method of using light-emitting diode (LEDs) to create white light (WLEDs) has been proposed and practiced in many different fields from industrial usage to aesthetic lighting application. The advantages of using LEDs, which are small dimensions, flexibility, durability, environmental friendliness, and saving on energy, have extended the scale of WLED application. The high demand of WLEDs for advanced technologies has led to a strong urge for WLED innovation and captured researchers' attention [1]-[3]. The WLEDs that have been currently commercially used consist of blue LEDs chips and the compound $Y_3Al_5O_{12}:Ce^{3+}$ ($YAG:Ce^{3+}$) phosphor and organic resins [4], [5]. This configuration of WLEDs was simple and had low manufacturing costs while still accomplishing an adequate level of performance but not suitable for lighting applications with higher demands. In particular, these conventional WLEDs showed high thermal discharge which lowered the working hours, changed the color temperature, affected light consistency, and projected less light with distorted light color after a period of time [6], [7]. The incompatible refractive index between 1.5 of $YAG:Ce^{3+}$ yellow phosphor and 1.8 of organic encapsulation became an obstacle that prevented the emitted light from being freely transferred out of the device, which caused part of the total light to be trapped and re-absorbed [8], [9].

Phosphor in-glass (PiG) with promising features such as durability, heat-generating consistency, and minimal expansion size from the heat was used to improve the flaws existing in applying organic substances [10]-[15]. The phosphor in-glass is formed by combining glass powders and phosphor particles at temperatures lower than 800 °C and then placed in WLEDs as a light transmission layer. Moreover, the refractive index of PiG can be modified to be compatible by combining more polarizable-ion with the precursor of the glass matrix. Through applying screen-printing and low-temperature sintering to integrate yellow YAG:Ce^{3+} phosphor with borosilicate glass, a PiG with YAG:Ce^{3+} traits was created in the previous study. The properties of the resulting light from this PiG were cool white light, 114 lm/W of LE, 5524 K correlated color temperature (CCT), and a color rendering index (CRI) of 69 [16], [17]. Despite good lighting efficiency, higher CRI (for example, over 85) in YAG:Ce^{3+} PiG was somehow difficult to obtain. To achieve high CRI, it requires high red light intensity in the lighting spectra to balance the primary color distribution, yet the YAG:Ce^{3+} PiG did not provide the red color pattern to the spectral zone, leading to low CRI as well as poor lighting quality. In order to address this issue, CaAlSiN$_3$:Eu^{2+} (CASN:Eu^{2+}) was proposed to be added into the PiG for increasing red light components [18], [19]. However, adding red phosphor might not be the most efficient solution since the characteristics of a red phosphor, including the thermal degradation and the interaction with the surface of the glass matrix, can be detrimental to light-emitting efficiency of red CaAlSiN$_3$:Eu^{2+} (CASN:Eu^{2+}) phosphor. Not to mention, flat surface PiG also reduced total emitted light because the discrepancy between the PiG and environment increased total internal reflection (TTR) and caused more radiations to be reflected to the chip package. A solution of engraving patterned at microscopic or nano size onto the package was introduced to reduce the light loss and led to numerous lithography methods from photoresist reflow, direct laser writing, to inkjet imprinting to be applied. However, there was a trade-off in using each solution, for example, the photolithographic technique would consume too much time to operate and also result in mass pollution. Direct laser writing with impeccable accuracy can create quality patterns, however, its cost was too much, so should not be considered for mass production. Inkjet printing created mask-less lithography, offered cost efficiency, and was suitable for serial production but not an ideal method due to inconsistent pattern and unsuitable size. As a result, finding an optimal fabrication method for a YAG:Ce^{3+} PiG structure with affordable prices and high light emission rate and chromatic performance is still unattainable.

To the best of our knowledge, a remote phosphor structure could address the cost and light emission issues, but the chromatic performance was not improved. Hence, we tried to apply a dual-layer phosphor (DLP) design to the remote phosphor structure (RPS), in which another phosphor film was placed the yellow phosphor YAG:Ce^{3+}, to enhance the color homogeneity. Though the DLP configuration could stimulate color uniformity, there still exist drawbacks in luminous flux (LF), which results in the idea of using three layers of different phosphors with different emission colors to get a more uniform chroma performance with efficient lumen strength. The assumption is the triple-layer phosphor (TLP) has better optical performances than the dual-layer. However, to fabricate an optimal TLP structure, the concern is not only focused on the concentration of added red and green phosphors but also on the distance between the phosphor layers and the other components in the package. In this paper, we conducted experiments to prove the benefits of TLP structures, and in terms of the distance among the phosphor layers, we will discuss this in another article.

Through the study of the TLP structure that consists of yellow YAG:Ce^{3+}, green Zn$_2$SiO$_4$:Mn^{2+},As^{5+}, and red YAl$_3$B$_4$O$_{12}$:Eu^{3+} phosphor layers, we can demonstrate the impacts of this structure on achieving the aforementioned target. The manuscript will provide vital content for references that are useful for WLED manufacturers. In the next sections, the study will be organized as shown in. Section 2 is for related works, in which we will demonstrate why we decide to work on a triple-layer remote phosphor layer for better WLED quality. In section 3, the phosphor preparation of yellow, green, and red phosphor used in the experiments, and the WLED simulation carried out with LightTools software are presented in detail. Section 4 is the presentation of scattering computation, comparison, and discussion of the CRI, CQS, and LF performances of the DLP and TLP structures. The conclusion or summary on the utility of the TLP remote structure is in section 5.

2.   RELATED WORKS

Various improvements were made to the remote phosphor structures to enhance their lighting properties. The concept of using a multi-layer remote phosphor design was implemented and resulted in noticeable enhancements in lumen output and chromatic properties of WLEDs. Adnan *et al*. [20] pointed out the efficiency in the luminescence of dual-layer remote phosphor structure increased by 5%, and lower chromatic deviation, in comparison with the conventional remote phosphor structure. Separating the red and yellow phosphor in the remote structure also achieved an 18% enhancement in luminous flux and effectively decreased the junction temperature; while its color shift is the same as the red-yellow-phosphor-mixed structure [21]-[23]. Yet, the color parameter and the effects of the specific red phosphors used in the dual-

layer structure were not deeply investigated in these studies. We cooperated with other researchers to analyze the effects of red phosphor $CaMgSi_2O_6:Eu^{2+},Mn^{2+}$ in the dual-layer structure. The results showed that this phosphor can result in higher CRI and CQS but a reduction in LF when being applied with a high concentration. However, the luminous flux was still better than using a single-layer remote phosphor that mixed the $CaMgSi_2O_6:Eu^{2+},Mn^{2+}$ into the yellow phosphor layer [24]. Besides, green phosphors were applied to enhance the performance of WLEDs. $SrBaSiO_4:Eu^{2+}$, a favorable commercial phosphor, was put on the yellow-emitting film with different concentrations. The higher concentration of $SrBaSiO_4:Eu^{2+}$ heightened the luminous flux and lowered the color deviation, yet degraded the CRI [25]. Here, we see that the red phosphor is beneficial to the CRI while the green phosphor is good for the luminous flux. Besides, the dual-layer structure somehow cannot manage to attain both high color rendering index and high lumen output simultaneously. Therefore, we decided to combine both red and green phosphor to fabricate a new RPS. The TLP structure, in which the phosphor layer of green-emitting phosphors is beneath that of red-emitting phosphors and the yellow-emitting phosphor film, can take advantage of the benefits from the green and red phosphors to perform better color quality and luminous efficiency for WLED packages. In this study, we will present the changes in WLED optical properties of TLP structure. We also present a comparison of the results from TLP and DLP structures to provide more evidence on the benefits of triple-layer remote phosphor on future WLED developments.

3. RESEARCH METHOD

3.1. Preparation of phosphor materials

The preparation of yellow $Y_3Al_5O_{12}:Ce^{3+}$ (YAG:Ce^{3+}) red $YAl_3B_4O_{12}:Eu^{3+}$ and green $Zn_2SiO_4:Mn^{2+},As^{5+}$ phosphors plays an indispensable role in building the experimented WLED remote phosphor structures. The chemical compositions for these phosphors are presented in Tables 1-3. The ingredients of yellow phosphor composition are mixed in water to form a slurry. Then this slurry is fired at 1,300 °C for an hour in a capped quartz tube filled with CO, followed by a powdering step. 2.7 g NH_4Cl will be added and mixed with the powder by dry grinding. After that, this mixture is fired two more times at 1,300 °C. Particularly, the first time, it will be heated up in capped quartz tubes with CO for 2 hours, and subsequently powdered. The second time, the firing process will be carried out in open quartz tubes with CO for 1 hour. The attained $Y_3Al_5O_{12}:Ce^{3+}$ has an emission color of yellow-green with an emission peaking at 2.37 eV, and its emission width is about 0.45 eV.

Table 1. Chemical composition of yellow phosphor $Y_3Al_5O_{12}:Ce^{3+}$ (YAG:Ce^{3+})

Ingredient	Mole%	By weight (g)
Y_2O_3	35.5 (of Y)	40
Al_2O_3	62.5 (of Al)	32
CeO_2	2	3.44
NH_4Cl	5	2.7

The fabrication process of green phosphor $Zn_2SiO_4:Mn^{2+},As^{5+}$ consists of 3 steps. First, combine all the ingredients by ball-milling them in water for 2 hours. Second, the mixture is dried in air and powdered subsequently. Finally, fire the resulting powder in a capped quartz tube at 1,200°C for an hour. The final product should have a peak emission of 2.35 eV and emits a green color spectrum.

Table 2. Chemical composition of green phosphor $Zn_2SiO_4:Mn^{2+},As^{5+}$

Ingredient	Mole%	By weight (g)
ZnO	200	163
$MnCO_3$	0.2	0.230
SiO_2	102	62.1
As_2O_3	0.02 (of As)	0.02

The fabrication process of red phosphor $YAl_3B_4O_{12}:Eu^{3+}$ starts with a blending step, includes 4 stages of firing, and ends with a washing step to remove residue. In the first step, the ingredients are mixed by being ground together. Then, in the next 4 steps, the mixture is fired for an hour and ground into powder at the end of each step. It is noted that the first firing is conducted at 500 °C in open quartz tube, while the other three are carried out in an open alumina crucible and at 900 °C, 1,100 °C, and 1,200 °C, respectively. After the fourth firing process is finished, wash the completed product with hot water several times and then

leave it dry. The completed product should have red color emission with emission peaks at 2.01 and 2.035 eV.

Table 3. Chemical composition of red phosphor $YAl_3B_4O_{12}:Eu^{3+}$

Ingredient	Mole%	By weight (g)
Y_2O_3	90 (of Y)	102
Eu_2O_3	10 (of Eu)	17.6
Al_2O_3	300 (of Al)	153
H_3BO_3	410	248

3.2. Simulation process

The cross-section images of multi-layer WLED subjects used in the experiment are presented in Figure 1. The Figures 1(a) and (b) depicting WLED devices with double-layer and triple-layer phosphor settings (DLP and TLP), respectively. These figures also demonstrate the arrangement of components inside the WLED: a half-dorm on top covers all the components, the chromatic phosphor layers with a thickness of 0.08 mm are placed in the order of red, green, and yellow, while the blue square cubes present the LEDs chips are attached to the substrate. The blank spaces between the components are silicone gel joining them together. The substrate used in the structure is aluminum nitride, the yellow phosphor is $YAG:Ce^{3+}$, and the color temperature is 5,600 K when viewing from the z-axis.

To ensure the calculation is accurate, the color temperature must be consistent when the phosphor weight percentages (wt%) of $YAl_3B_4O_{12}:Eu^{3+}$ and $Zn_2SiO_4:Mn^{2+},As^{5+}$ increase. Therefore, the decline in yellow $YAG:Ce^{3+}$ proportion is essential to achieve this goal. As a result, the amounts of $YAG:Ce^{3+}$ at different ACCTs vary and cause the light scattering and optical properties to change. Figure 2 exhibits in detail the correlation between $YAG:Ce^{3+}$ and ACCTs within two WLED devices with DLP and TLP settings. In Figure 2(a), the phosphor $YAG:Ce^{3+}$ percentage at all CCT values in the DLP is greater than in the TLP. $YAG:Ce^{3+}$ with high concentration could initiate a higher probability of light loss owing to the increasing back-scattered lights. Eventually, the light proportion that can be emitted from the WLED decreases, in other words, the LF is reduced. Besides, the reproducing color quality is degraded with such an excessive $YAG:Ce^{3+}$ concentration since the more the yellow phosphor concentration is applied, the more the yellow lights are generated, which finally causes the imbalance among the component color spectra forming white light, including yellow, blue, green, and red. In Figure 2(b) suggests that an excessively high proportion of yellow lights probably causes the WLED light to lean over the yellow color and initiate the yellow ring to appear on the object's surface.
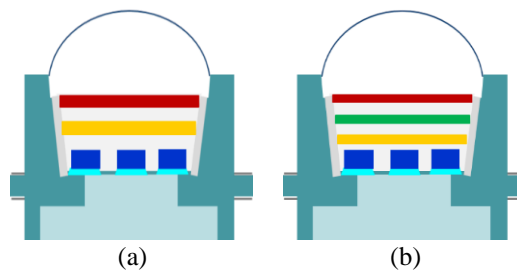
Figure 1. Pictures detailing the cross-sections of WLEDs with multiple layers (a) DLP and (b) TLP

From this hypothesis, limiting too much back-scattering events is a desirable solution for developing the efficiency of white lights. One of the approaches to get this solution is to heighten the red spectral energy, which can be successfully enriched by using red $YAl_3B_4O_{12}:Eu^{3+}$ phosphors. The red phosphor benefits the essential red-emission color for color rendition, as shown in Figure 3. On the other hand, the angular color uniformity (ACU) and LF can get better performances with improved green-emission color by utilizing green phosphor $Zn_2SiO_4:Mn^{2+},As^{5+}$. Based on the criteria of these solutions, using the TLP could bring desired results. However, for the practical use of the TLP configuration, its influences should be considered and assessed carefully, which is demonstrated in the following sections.
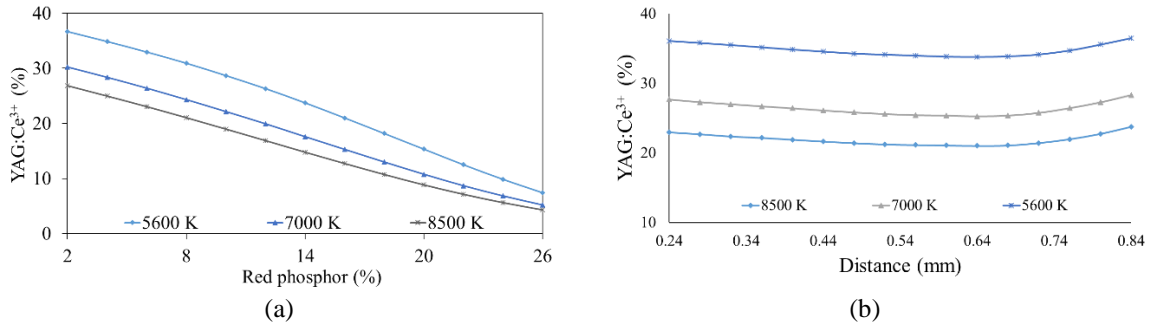
Figure 2. Concentration variation of yellow phosphor YAG:Ce^{3+} under different AACTs in two multi-layer WLEDs (a) DLP and (b) TLP
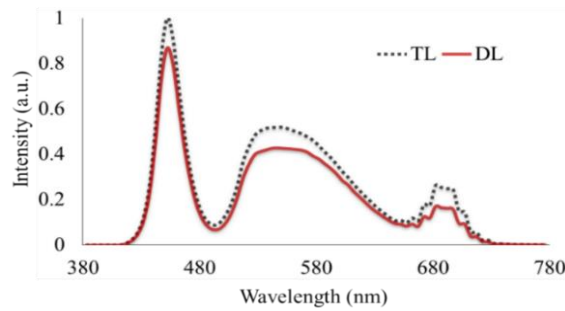
Figure 3. Emission spectra of the TLP and DLP at CCT 8,500 K

4. RESULTS AND DISCUSSION

After calculating CRI in each structure, the results are compared in Figure 4. From Figure 4(a), the dual-layer structure is superior to the triple-layer in terms of CRI at every applied color temperature in the experiment. In addition, the CRI was continuously rising from 5,600 K to 8,500 K color temperature. It has been noted that the improvement of CRI in phosphor-converted WLEDs with high color temperature (7,000 K) is extremely hard to achieve, yet the DL still yields high CRI at 8,500 K, which demonstrates that DL structure is appropriate to improve CRI in remote phosphor structure even in a structure with high color temperature, see Figure 4(b).

Moreover, the CRI of DLP structure, as depicted in Figure 4(a), shows a gradual improvement when the weight percentage of the red phosphor increases in 2–26 wt% range, which can be attributed to the provided red light components by the additional red phosphor layer YAl$_3$B$_4$O$_{12}$:Eu^{3+} in DLP structure. From this result, it can be confirmed that a DL structure with a red phosphor layer is optimal for WLEDs performing great CRI adequacy.
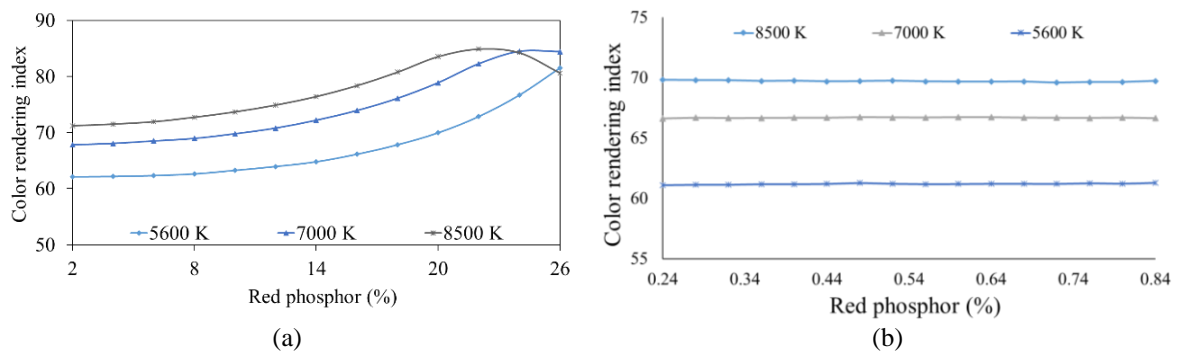
Figure 4. CRI performances corresponding to ACCTs in two multi-layer WLEDs (a) DLP and (b) TLP

Although the TLP structure is inferior to the DLP in terms of color rendering index, it excels in color quality scale (CQS), which is presented in Figure 5. As soon as the lighting industry expands, a requirement for a more advanced meter to evaluate lighting device performance has started to arise. The CRI is a valuable index but the scope of this quality indicator is limited and cannot fully examine the performance of a lighting device. Therefore, CQS, which combines CRI and two other aspects of viewers' preference and chromaticity coordinate, has become a greater goal for researchers to achieve. Based on this information, Figure 5, which shows TLP structure results in higher CQS value than DLP structure, has confirmed TLP structure has better color quality. The enhanced color quality in TLP structure is the result of added red and green phosphors that contribute much to keeping the balance between the three fundamental colors forming white light. In addition, the participation of green $Zn_2SiO_4:Mn^{2+},As^{5+}$ phosphor in the phosphor package also benefits the luminous flux of TLP remote phosphor structure.
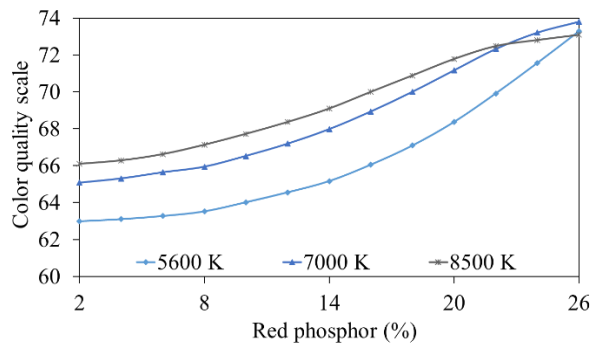
Figure 5. CQS performances of corresponding to ACCTs of DLP

From the content of Figure 5, it can be said that the TLP structure is the ideal choice for WLEDs focusing on color quality. However, the light output in WLEDs with high color quality is usually lower. This normal occurrence raised the question about how the luminous flux of TLP structure is affected if the chroma metrics are remarkably enhanced. Therefore, the luminescent output of both DLP structure and TLP structure are calculated and compared to answer this question and provide solution if such incident occurs. In this part, equations applied for the calculation of transmission and conversion factors of the blue and yellow lights, respectively, of the TLP structure are performed. The study of these values will expand our understanding of this structure and possibly offer an appropriate method to enhance WLED efficiency.

Computations for blue light transmission and yellow light conversion of the DLP package, which has the phosphor layer's thickness presented by h, are:

$$PB_2 = PB_0 e^{-2\alpha_{B_2}h} \tag{1}$$

$$PY_2 = \frac{1}{2}\frac{\beta_2 PB_0}{\alpha_{B_2}-\alpha_{Y_2}}[e^{-2\alpha_{Y_1}h} - e^{-2\alpha_{B_1}h}] \tag{2}$$

in the TLP structure, the phosphor film's thickness is $\frac{2h}{3}$, and the blue light transmission and yellow light conversion can be demonstrated by:

$$PB_3 = PB_0.e^{-\alpha_{B_2}\frac{2h}{3}}.e^{-\alpha_{B_2}\frac{2h}{3}}.e^{-\alpha_{B_2}\frac{2h}{3}} = PB_0.e^{-2\alpha_{B_3}h} \tag{3}$$

$$PY'_3 = \frac{1}{2}\frac{\beta_3 PB_0}{\alpha_{B_3}-\alpha_{Y_3}}[e^{-\alpha_{Y_3}\frac{2h}{3}} - e^{-\alpha_{B_3}\frac{2h}{3}}]e^{-\alpha_{Y_3}\frac{2h}{3}} + \frac{1}{2}\frac{\beta_3 PB_0 e^{-\alpha_{B_3}\frac{2h}{3}}}{\alpha_{B_3}-\alpha_{Y_3}}[e^{-\alpha_{Y_3}\frac{2h}{3}} - e^{-\alpha_{B_3}\frac{2h}{3}}]$$
$$= \frac{1}{2}\frac{\beta_3 PB_0}{\alpha_{B_3}-\alpha_{Y_3}}[e^{-\alpha_{Y_3}\frac{4h}{3}} - e^{-2\alpha_{B_3}\frac{4h}{3}}] \tag{4}$$

$$PY_3 = PY'_3.e^{-\alpha_{Y_3}\frac{2h}{3}} + PB_0.e^{-2\alpha_{B_3}\frac{4h}{3}}\frac{1}{2}\frac{\beta_3}{\alpha_{B_3}-\alpha_{Y_3}}[e^{-\alpha_{Y_3}\frac{2h}{3}} - e^{-\alpha_{B_3}\frac{2h}{3}}]$$
$$= \frac{1}{2}\frac{\beta_3 PB_0}{\alpha_{B_3}-\alpha_{Y_3}}[e^{-\alpha_{Y_3}h} - e^{-2\alpha_{B_3}h}] \tag{5}$$

In which subscripts as "2" and "3" show the DLP and TLP structures, in turn. β indicates the light conversion coefficients from blue to yellow, and γ indicates the yellow-light reflection coefficients. PB_0 is the blue-LED light intensity that comprises both blue-light intensity – PB and yellow-light intensity – PY. α_B is the energy-loss fraction of blue lights and α_Y is that of yellow lights. Besides, in (4), PY'_3 demonstrates the transmitted yellow lights that go through the other phosphor sheets in the TLP configuration.

The TLP structure can considerably stimulate the lighting efficiency (LE) of a WLED, more than the DLP, as implied from the following expression:

$$\frac{(PB_3-PY_3)-(PB_2+PY_2)}{(PB_2+PY_2)} > \frac{e^{-2\alpha_{B_3}h} - e^{-2\alpha_{B_2}h}}{e^{-2\alpha_{Y_3}h} - e^{-2\alpha_{B_2}h}} > 0 \tag{6}$$

the Mie-theory is used in the scattering analysis of phosphor particles and also in the computation of scattering cross section C_{sca} for spherical particles. The transmitted light power can be calculated by the Lambert-Beer law [25]:

$$I = I_0\ exp(-\mu_{ext}L) \tag{7}$$

from (6), we can conclude that more phosphor layers in the WLED package will result in more scattering events and enhance the luminous flux. Therefore, the TLP structure has outstanding LE, in comparison to the DLP structure. The advantage of the TLP structure is further shown in Figure 6, which depicts the correlation between lumen and ACCT levels in both DLP and TLP. As presented in Figure 6(a), the lumen output in TLP structure shows greater values than in DLP configuration at every color temperature point in the range of 5,600 K–8,500 K. That the TLP can yield better luminous efficiency than the DLP can be attributed to the higher emission spectra in the wavelength region of 500–600 nm due to the reduction of yellow YAG:Ce^{3+} phosphor concentration to maintain the color temperature, as can be seen in Figure 3. Moreover, the green spectral color is included in this wavelength band, which means the green emission is also boosted. Through Figure 6(b), it can be observed that when the lumen output is under control of green light components, the enhancement in green emission probably leads to better results. Additionally, this yellow-phosphor concentration reduction, combined with the ability to limit light loss from back-scattering of TLP structure, greatly promotes the light conversion rate from blue light to white light and allows more emitted lights to easily pass through the yellow phosphorus layer. So, in comparison with dual-layer structures, the emission intensity of the triple-layer structure on the white light emission wavelength band is higher, thus, creating more white lights. Apparently, a TLP structure with better performance in both CQS and lighting efficiency is more effective in enhancing the optical performance of WLEDs.
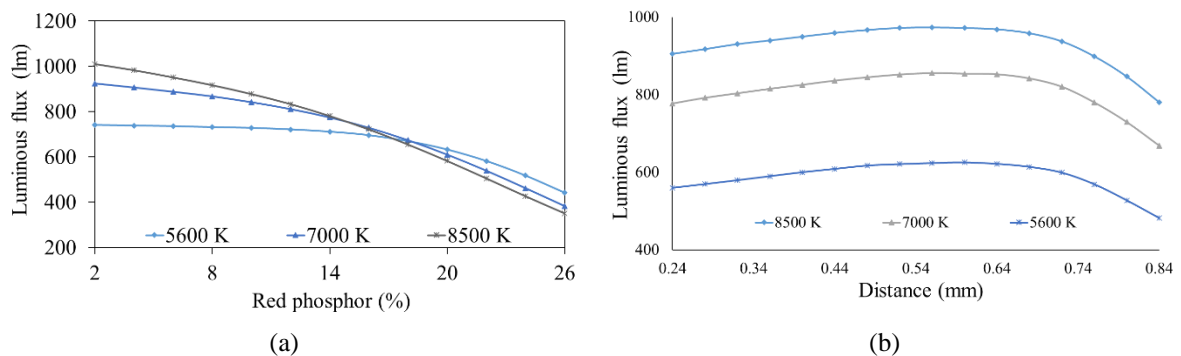
Figure 6. Variations of luminous flux performances corresponding to ACCTs in two multi-layer WLEDs
(a) DLP and (b) TLP

Back to the color quality aspect, besides the color quality scale, the color homogeneity is also a crucial value for WLED chromatic performance and has received much attention. Increasing the color uniformity has always been a priority for researchers when studying WLEDs, therefore, many methods were proposed to perfect this value, from adding SiO_2, $CaCO_3$ scattering enhancement particles to using an innovative coating method such as conformal diffusing. Applying these methods can enhance the color uniformity; however, the luminous flux is damaged in the process. On the other hand, using red

$YAl_3B_4O_{12}:Eu^{3+}$ and green $Zn_2SiO_4:Mn^{2+},As^{5+}$ phosphors can compensate for the lack of red and green lights needed for white light while preventing emitted light from reflecting back inside the package. Only the phosphor concentration needed to be modified correctly for the optimal performnaces, which can be referred to the Lambert-Beer law in (7). The color deviation values, which can be seen from Figure 7, show the better consistency in the TLP structure than in the DLP structure, owing to the lower color deviation of TLP configuration. That the color uniformity of the TLP increases and becomes more noticeable at higher ACCTs is a result of more scattering events created from the phosphor layers. The downside of more scattering events is that it might reduce the light output, which has occurred in this case. However, the decreased luminous flux is not much and is mostly outweighed by the reduced light loss from back-scattering. Therefore, the TLP structure is still an optimal structure in WLED optical properties' enhancement.
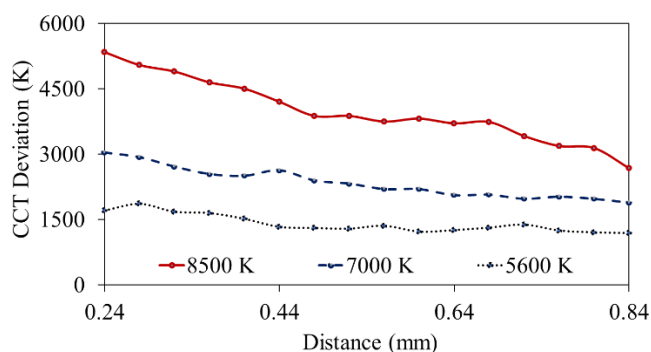
Figure 7. Chromatic deviation (D-CCT) corresponding to ACCTs of TLP

5. CONCLUSION

The comparison of optical influences between DLP structure and TLP structure at different ACCTs has led to a conclusion that the TLP structure is a more advanced structure for lighting performance improvement. The Mie theory and the Lambert-Beer law are applied to ensure the accuracy of experimental results. The added phosphor layers in TLP structure are effective tools for enhancing optical properties. Particularly, the green phosphor $Zn_2SiO_4:Mn^{2+},As^{5+}$ benefits color uniformity and luminous flux, and $YAl_3B_4O_{12}:Eu^{3+}$ red phosphor can improve the CRI and CQS of the WLED package. As a result, TLP remote phosphor structure is excellent in luminous flux, color uniformity, and CQS. In other words, the TLP structure, with three chromatic phosphor layers can enhance lumen output and color quality simultaneously, a result that cannot be achieved with DLP structure. Meanwhile, the DLP structure has a higher CRI than the TLP structure, thus, this structure is suitable for the production of WLEDs that need high CRI. Based on these findings, manufacturers can choose an appropriate structure for their production targets and enhance the performance of WLED packages.

REFERENCES

[1] P. Zhu, H. Zhu, G. C. Adhikari, and S. Thapa, "Design of circadian white light-emitting diodes with tunable color temperature and nearly perfect color rendition," *OSA Continuum*, vol. 2, no. 8, p. 2413, Aug. 2019, doi: 10.1364/osac.2.002413.
[2] S. Beldi *et al*., "High Q-factor near infrared and visible Al 2 O 3 -based parallel-plate capacitor kinetic inductance detectors," *Optics Express*, vol. 27, no. 9, p. 13319, Apr. 2019, doi: 10.1364/oe.27.013319.
[3] N. C. A. Rashid *et al*., "Spectrophotometer with enhanced sensitivity for uric acid detection," *Chinese Optics Letters*, vol. 17, no. 8, p. 081701, 2019, doi: 10.3788/COL201917.081701.
[4] C.-H. Lin *et al*., "Hybrid-type white LEDs based on inorganic halide perovskite QDs: candidates for wide color gamut display backlights," *Photonics Research*, vol. 7, no. 5, p. 579, May 2019, doi: 10.1364/prj.7.000579.
[5] S. K. Abeysekera, V. Kalavally, M. Ooi, and Y. C. Kuang, "Impact of circadian tuning on the illuminance and color uniformity of a multichannel luminaire with spatially optimized LED placement," *Optics Express*, vol. 28, no. 1, p. 130, Jan. 2020, doi: 10.1364/oe.381115.
[6] F. Arena and G. Pau, "An overview of big data analysis," *Bulletin of Electrical Engineering and Informatics*, vol. 9, no. 4, pp. 1646–1653, Aug. 2020, doi: 10.11591/eei.v9i4.2359.
[7] G. E. Romanova, V. I. Batshev, and A. S. Beliaeva, "Design of an optical illumination system for a tunable source with acousto-optical filtering," *Journal of Optical Technology*, vol. 88, no. 2, p. 66, Feb. 2021, doi: 10.1364/jot.88.000066.

[8] L. V. Labunets, A. B. Borzov, and I. M. Akhmetov, "Regularized parametric model of the angular distribution of the brightness factor of a rough surface," *Journal of Optical Technology*, vol. 86, no. 10, p. 618, Oct. 2019, doi: 10.1364/jot.86.000618.

[9] Y. J. Park *et al*., "Development of high luminous efficacy red-emitting phosphor-in-glass for high-power LED lighting systems using our original low Tg and Ts glass," *Optics Letters*, vol. 44, no. 24, p. 6057, Dec. 2019, doi: 10.1364/ol.44.006057.

[10] G. Prabhakar, P. Gregg, L. Rishoj, P. Kristensen, and S. Ramachandran, "Octave-wide supercontinuum generation of light-carrying orbital angular momentum," *Optics Express*, vol. 27, no. 8, p. 11547, Apr. 2019, doi: 10.1364/oe.27.011547.

[11] M. Quesada *et al*., "All-glass, lenticular lens light guide plate by mask and etch," *Optical Materials Express*, vol. 9, no. 3, p. 1180, Mar. 2019, doi: 10.1364/ome.9.001180.

[12] M. Royer, "Evaluating tradeoffs between energy efficiency and color rendition," *OSA Continuum*, vol. 2, no. 8, p. 2308, Aug. 2019, doi: 10.1364/osac.2.002308.

[13] A. Ahmad, A. Kumar, V. Dubey, A. Butola, B. S. Ahluwalia, and D. S. Mehta, "Characterization of color cross-talk of CCD detectors and its influence in multispectral quantitative phase imaging," *Optics Express*, vol. 27, no. 4, p. 4572, Feb. 2019, doi: 10.1364/oe.27.004572.

[14] S. Bindai, K. Annapurna, and A. Tarafder, "Realization of phosphor-in-glass thin film on soda-lime silicate glass with low sintering temperature for high color rendering white LEDs," *Applied Optics*, vol. 58, no. 9, p. 2372, Mar. 2019, doi: 10.1364/ao.58.002372.

[15] S. Feng and J. Wu, "Color lensless in-line holographic microscope with sunlight illumination for weakly-scattered amplitude objects," *OSA Continuum*, vol. 2, no. 1, p. 9, Jan. 2019, doi: 10.1364/osac.2.000009.

[16] W.-Y. Chang, Y. Kuo, Y.-W. Kiang, and C. C. Yang, "Simulation study on light color conversion enhancement through surface plasmon coupling," *Optics Express*, vol. 27, no. 12, p. A629, Jun. 2019, doi: 10.1364/oe.27.00a629.

[17] K. Orzechowski, M. M. Sala-Tefelska, M. W. Sierakowski, T. R. Woliński, O. Strzeżysz, and P. Kula, "Optical properties of cubic blue phase liquid crystal in photonic microstructures," *Optics Express*, vol. 27, no. 10, p. 14270, May 2019, doi: 10.1364/oe.27.014270.

[18] H. Li *et al*., "Electrically driven, polarized, phosphor-free white semipolar (20-21) InGaN light-emitting diodes grown on semipolar bulk GaN substrate," *Optics Express*, vol. 28, no. 9, p. 13569, Apr. 2020, doi: 10.1364/oe.384139.

[19] J. Li, D. Han, J. Zeng, J. Deng, N. Hu, and J. Yang, "Multi-channel surface plasmon resonance biosensor using prism-based wavelength interrogation," *Optics Express*, vol. 28, no. 9, p. 14007, Apr. 2020, doi: 10.1364/oe.389226.

[20] A. Adnan, Y. Liu, C.-W. Chow, and C.-H. Yeh, "Demonstration of non-Hermitian symmetry (NHS) serial-complex-valued orthogonal frequency division multiplexing (SCV-OFDM) for white-light visible light communication (VLC)," *OSA Continuum*, vol. 3, no. 5, p. 1163, May 2020, doi: 10.1364/osac.391483.

[21] M. Lecca, "Generalized equation for real-world image enhancement by Milano Retinex family," *Journal of the Optical Society of America A*, vol. 37, no. 5, p. 849, May 2020, doi: 10.1364/josaa.384197.

[22] R. Dang, H. Tan, N. Wang, G. Liu, F. Zhang, and X. Song, "Raman spectroscopy-based method for evaluating LED illumination-induced damage to pigments in high-light-sensitivity art," *Applied Optics*, vol. 59, no. 15, p. 4599, May 2020, doi: 10.1364/ao.379398.

[23] S. Ma, P. Hanselaer, K. Teunissen, and K. A. G. Smet, "Effect of adapting field size on chromatic adaptation," *Optics Express*, vol. 28, no. 12, p. 17266, Jun. 2020, doi: 10.1364/oe.392844.

[24] D. Yan, S. Zhao, H. Wang, and Z. Zang, "Ultrapure and highly efficient green light emitting devices based on ligand-modified CsPbBr 3 quantum dots," *Photonics Research*, vol. 8, no. 7, p. 1086, Jul. 2020, doi: 10.1364/prj.391703.

[25] A. Ali *et al*., "Blue-laser-diode–based high CRI lighting and high-speed visible light communication using narrowband green-/red-emitting composite phosphor film," *Applied Optics*, vol. 59, no. 17, p. 5197, Jun. 2020, doi: 10.1364/ao.392340.

BIOGRAPHIES OF AUTHORS

Thanh Binh Ly 🆔 🔢 SC Ⓟ received an Environmental Engineering Technology Master degree from the Industrial University of Ho Chi Minh City, in 2020. Currently, He is research Industrial University of Ho Chi Minh City, Vietnam. Her research interests include simulation LEDs material, renewable energy. She can be contacted at email: lythanhbinh@iuh.edu.vn.

Phan Xuan Le 🆔 🔢 SC Ⓟ received a Ph.D. in Mechanical and Electrical Engineering from Kunming University of Science and Technology, Kunming city, Yunnan province, China. Currently, He is a lecturer at the Faculty of Engineering, Van Lang University, Ho Chi Minh City, Vietnam. His research interests are Optoelectronics (LED), Power transmission and Automation equipment. He can be contacted at email: le.px@vlu.edu.vn.